Environment International 215 (2026) 110478

Contents lists available at ScienceDirect

Environment International

journal homepage: www.elsevier.com/locate/envint

Full length article

# The extractive classroom: indoor school environments as reservoirs of mining legacy

Nicolás C. Zanetta-Colombo [a,b,*], Manuel Prieto [c,d,**], Carlos A. Manzano [e,f,***], Zoë L. Fleming [g], Manuel Leiva [e], Javiera Machuca [a], Lara Nigro [h], Camilla Della Torre [h], Anja Eichler [i,j], Petrus le Roux [k], Johanna R.C. Von Holdt [l], Alexander Varychev [m], Lucie Tajcmanova [n], Leah Chibwe [o], Javier A. Sánchez-Moreno [o], Christian Scholz [m], Stefan Rheinberger [m], Paola Rubilar [p], Estela Blanco [q,r], Josefa Alarcon-Paredes [e], Dagmar Brombierstäudl [s], Benoit Nemery [t], Luca Del Giacco [h], Alberto Diana [h], Marcus Nüsser [a,b]

[a] Department of Geography, South Asia Institute, Heidelberg University, Heidelberg, Germany
[b] Heidelberg Center for the Environment (HCE), Heidelberg University, Heidelberg, Germany
[c] Millennium Nucleus in Andean Peatlands (AndesPeat), Arica, Chile
[d] Departamento de Ciencias Históricas y Geográficas, Universidad de Tarapacá, Arica, Chile
[e] Departamento de Química, Facultad de Ciencias, Universidad de Chile, Santiago, Chile
[f] School of Public Health, San Diego State University, San Diego, CA, USA
[g] Centro de Investigación en Tecnologías para la Sociedad, Facultad de Ingeniería, Universidad del Desarrollo, Santiago, Chile
[h] Department of Biosciences, University of Milan, Milan, Italy
[i] PSI Center for Energy and Environmental Sciences, Paul Scherrer Institute, Villigen PSI, Switzerland
[j] Oeschger Centre for Climate Change Research, University of Bern, Bern, Switzerland
[k] Department of Geological Sciences, University of Cape Town, Cape Town, South Africa
[l] Department of Environmental and Geographical Sciences, University of Cape Town, Cape Town, South Africa
[m] Institute of Earth Sciences, Heidelberg University, Heidelberg, Germany
[n] Institute of Petrology and Structural Geology, Faculty of Science, Charles University, Prague, Czech Republic
[o] Institute for Environmental Change and Society, University of Regina, Regina, Saskatchewan, Canada
[p] Centro de Epidemiología y Políticas de Salud, Facultad de Medicina Clínica Alemana, Universidad del Desarrollo, Santiago, Chile
[q] College UC & Escuela de Salud Pública, Pontificia Universidad Católica de Chile, Santiago, Chile
[r] Center for Climate and Resilience Research (CR2), Santiago, Chile
[s] Institute of Environmental Social Sciences and Geography, University of Freiburg, Freiburg, Germany
[t] Centre for Environment and Health, Department of Public Health and Primary Care, KU Leuven, Leuven, Belgium

ARTICLE INFO

*Keywords:*
Chile
Copper mining
Indoor pollution
Environmental Justice
Extractive classroom
Just Transition

ABSTRACT

The global energy transition is accelerating the demand for copper and other energy-transition minerals worldwide, potentially expanding the existing large-scale mining across the Global South. Sustainability assessments of mining currently focus primarily on ambient outdoor concentrations of chemicals (metals) and commonly assume that buildings can buffer human exposure. Here we test this assumption in Calama, Chile, a desert city downwind of one of the world's largest copper-mining complexes (Chuquicamata). We combined elemental, isotopic, and mineralogical analyses with oxidative potential measurements and zebrafish embryo assays to examine paired indoor and outdoor settled dust from 38 schools in Calama. Indoor concentrations of Cu, As, Pb, and Mo closely tracked outdoor levels and exceeded regional desert background by up to one order of magnitude, with minimal attenuation for As and Pb. Mineralogical and isotopic evidence indicated that the dust is not connected to fresh vehicles or combustion emissions, but rather to the mining industry. Additionally, the

* Corresponding author at: Department of Geography, South Asia Institute, Heidelberg University, Heidelberg, Germany.
** Corresponding author at: Millennium Nucleus in Andean Peatlands (AndesPeat), Arica, Chile.
*** Corresponding author at: Departamento de Química, Facultad de Ciencias, Universidad de Chile, Santiago, Chile.
*E-mail addresses:* nicolas.zanetta@sai.uni-heidelberg.de (N.C. Zanetta-Colombo), mprieto@academicos.uta.cl (M. Prieto), Carlos.manzano@uchile.cl (C.A. Manzano).

https://doi.org/10.1016/j.envint.2026.110478
Received 1 June 2026; Received in revised form 17 August 2026; Accepted 20 August 2026
Available online 28 August 2026
0160-4120/© 2026 The Author(s). Published by Elsevier Ltd. This is an open access article under the CC BY license (http://creativecommons.org/licenses/by/4.0/).

evidence showed enrichment in oxidized mining-derived particles, and indoor dust exhibited substantial oxidative potential. Zebrafish embryos exposed to dust extracts showed elevated heart rate under sublethal conditions. These results indicate that indoor environments in intensive mining landscapes, including classrooms, may be physically integrated into the surrounding extractive environment and should be incorporated into regular environmental monitoring, mine-closure planning, and just-transition governance.

## 1. Introduction

The global transition towards low-carbon energy systems is increasing the demand for mineral resources (Hund et al., 2023; IEA, 2021; Vidal et al., 2013; Watari et al., 2019). Meeting these requirements will need a substantial expansion of the existing mining activities, particularly in regions that already host ore deposits and extraction infrastructure. Many of these regions are located in the Global South, where mineral production plays a central role in national economies and global supply chains (Sovacool et al., 2020). However, the environmental and social costs associated with extraction remain unevenly distributed, disproportionally affecting communities that live near mines and smelters (Ali et al., 2017; Bebbington et al., 2018).

Efforts to ensure that mineral supply chains align with sustainability objectives have expanded in recent years (Azapagic, 2004; Sovacool et al., 2020). Nevertheless, most sustainability assessments of mining continue to focus on landscape-scale disturbances such as land transformation, water consumption, tailing management, and greenhouse-gas emissions. Air pollution from mining is typically evaluated through outdoor metrics such as suspended dust concentrations or metal deposition measured at fixed monitoring stations. Outdoor dust can infiltrate buildings through ventilation systems, open windows, and structural gaps. Once indoors, it may accumulate on surfaces, be resuspended, or be transported on clothing, footwear, and personal objects (Layton & Beamer, 2009; Leppänen et al., 2020; Morawska et al., 2017; Nazaroff, 2016). Studies on school environments have shown that indoor dust concentrations often reflect the proximity to pollution sources and can remain elevated despite compliance with outdoor air-quality standards (Rivas et al., 2014; Sadrizadeh et al., 2022).

Mining activities generate large volumes of mineral dust whose composition differs substantially from urban traffic aerosols. Dust produced during ore extraction, crushing, transport, and tailings weathering often contains elevated concentrations of metals such as Cu, As, and Pb (Csavina et al., 2012; Plumlee et al., 2006). In arid environments, these dust particles can remain mobile for long periods due to limited rainfall, strong winds, and extensive disturbed surfaces (Morman & Plumlee, 2014). Additionally, weathering of ore and smelter residues also produce secondary mineral phases, including metal oxides and oxysalts, which have been demonstrated to increase the mobility and chemical reactivity of toxic metals (Ettler, 2016).

A growing body of epidemiological research links air pollution in school environments with respiratory illness, impaired lung development, and reduced cognitive performance in children (Clark et al., 2012; Gilraine & Zheng, 2024; Sunyer et al., 2015). The health implications of exposure to metal-rich dust are well documented. Metals including Pb and As are potent neurotoxins associated with impaired cognitive development and long-term neurological damage in children (Bellinger, 2013; Grandjean & Landrigan, 2014; Lanphear et al., 2005). Other metals can catalyse redox reactions that generate reactive oxygen species and oxidative stress, processes linked to cardiovascular and respiratory diseases (Charrier & Anastasio, 2012; Kelly & Fussell, 2015). Children are particularly vulnerable to such exposures because of their higher inhalation rates relative to body mass, frequent hand-to-mouth contact with soil and dust, and ongoing neurological development (Cohen et al., 2024; Landrigan et al., 2018). Schools can therefore represent critical environments for understanding how mining derived dust intersects with child health and educational outcomes.

Previous studies in northern Chile have shown that soils and outdoor dust in mining cities are enriched in Cu, As, and Pb relative to regional background levels and reflect mixtures of natural and industrial sources (Zanetta-Colombo et al., 2022, 2024). Yet indoor environments, particularly schools, remain largely absent from environmental monitoring programs and sustainability assessments. Here we investigated paired indoor and outdoor surface dust samples from 38 schools in Calama, a city within northern Chile's Atacama Desert and located downwind of one of the world's largest copper-mining complexes. We combined elemental analyses with stable C and N isotopes, and radiogenic Pb isotopes to examine the origin of dust components. Single-particle mineralogy was used to characterize metal-bearing phases, while oxidative potential measurements assessed the redox activity of dust mixtures. Finally, zebrafish embryo assays provided preliminary evidence on whether classroom dust extracts can induce sublethal physiological responses in a vertebrate model.

## 2. Methods

### 2.1. Study design and sampling area

This study was initiated following a request from the Medical College of Calama for an independent environmental assessment of school-based metal exposure. In coordination with the municipal government, the research team contacted school principals to establish a sampling schedule. Sampling was conducted between January 7th and 14th, 2023. Thirty-eight schools from Calama were included in the study (Fig. 1). Each school was visited once, and paired indoor and outdoor settled dust samples were collected during the same visit. Fieldwork teams were divided into indoor and outdoor groups, each with at least three researchers and a designated school representative providing access to selected building areas. In each school, indoor teams collected surface dust from 5 to 10 classrooms per school, stratified by floor level, building orientation, and exposure to prevailing winds from nearby mining and industrial areas. Indoor dust samples were collected from multiple horizontal surfaces within each classroom, including student desktops, window ledges, bookshelves, and storage cabinets, prioritizing surfaces less frequently cleaned. Outdoor teams sampled perimeters and courtyards using the same protocol, collecting dust from benches, railings, outdoor tables, playground equipment, and building ledges. Dust was collected from existing surfaces under normal classroom operating conditions rather than following a defined accumulation period. Consequently, the duration over which dust accumulated before sampling is unknown and may vary among schools. All indoor and outdoor subsamples were pooled into a single indoor and outdoor composite per school, yielding 38 paired samples (76 in total). Team members wore nitrile gloves and protective masks during sampling, and new synthetic brushes (rinsed with deionized water between sites) and airtight polypropylene containers were used for each site. A field log was used to record the school's name, sampling time, and contextual factors.

A regional background control site (located in the Alto El Loa, over 50 km NE of Calama) was included for comparisons. This site was described in previous studies as showing an equilibrium background concentration for multiple elements indicated by a stabilization in variance beyond the final breakpoint of exponential decay models (Zanetta-Colombo et al., 2024). Dust collected at this site therefore represents regional background conditions with minimal industrial influence and was used as a reference across geochemical and toxicological analyses.

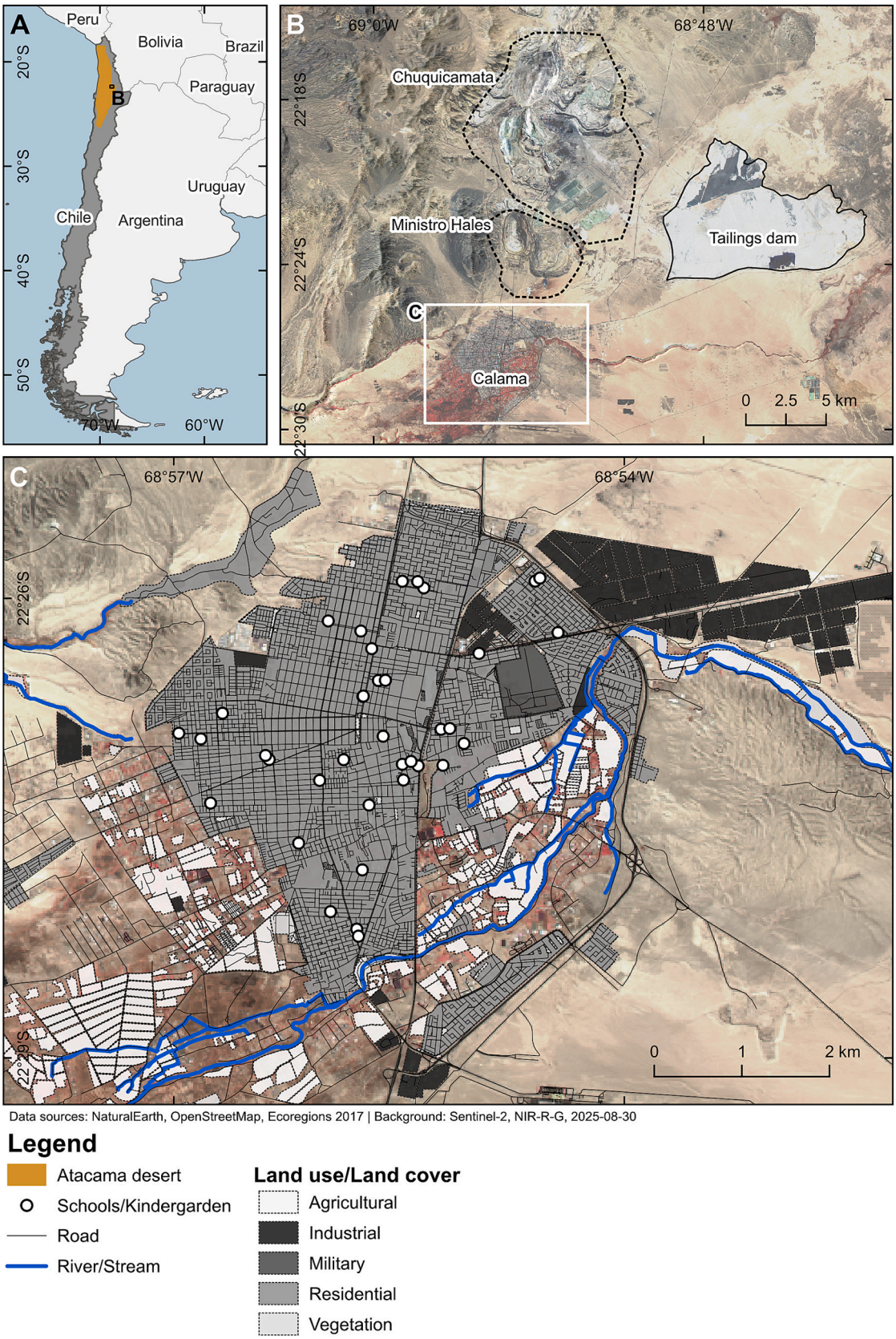


**Fig. 1.** (a) Chile within South America and the Atacama Desert in northern Chile. (b) Spatial setting of Calama, highlighting its proximity to the Chuquicamata and Ministro Hales copper mines and to the Talabre tailings deposit. (c) Land use and land cover of Calama, showing the spatial distribution of the 38 public schools included in the study.

No standardized survey of window and door opening, mechanical ventilation, classroom occupancy, or cleaning frequency was conducted across schools. These operational characteristics were therefore not included as explanatory covariates.

### 2.2. Sample preparation

Dust samples were transported to the Universidad del Desarrollo (Santiago, Chile) for preparation. Samples were sieved to the < 75 μm fraction, which is commonly used to characterize indoor settled dust and children's potential exposure through surface contact, incidental ingestion, and resuspension. Particle-size distributions within this fraction were not determined. Stainless-steel sieves were rinsed with ultrapure water after each sample to prevent cross-contamination. The < 75 μm fractions were sent to collaborating laboratories: Heidelberg University (Germany) for elemental and mineralogical analyses, University of Regina (Canada) for $\delta^{13}C$ and $\delta^{15}N$, University of Cape Town (South Africa) for Pb-isotope analysis, University of Milan (Italy) for zebrafish assays, and the Universidad de Chile for oxidative-potential analysis.

### 2.3. Elemental analysis (ICP-OES)

Dust samples (100 mg) were acid extracted using an ultraclave digestion system (MLS GmbH, Leutkirch, Germany) with 1.5 ml of $HNO_3$ (65% double sub-boiled) and 100 μl of $H_2O_2$ for 3 h at 240°C and 50 bar in Teflon digestion vessels. The resulting extracts were diluted to 10 ml with Milli-Q water. All samples were extracted in duplicate. The soil reference material BAM-U-115 (Aqua Regia Extractable Trace Elements in Soil, BAM, Germany) was extracted along samples ($n = 6$) for quality control. The elemental contents of the acid extracts were determined by ICP-OES analyses using a 720 ICP-OES from Agilent (Victoria, Australia) with a Conical® nebulizer and a cyclone chamber as the sample introduction system. All samples were measured in a 10-fold dilution. The wavelengths used to determine the individual elements, and the corresponding limits of quantification (LOQ) are given in Table S1. Aqueous reference materials (SPS-SW1, SPS-SW2, and TMDA61.3) were used for quality control and showed recovery rates that ranged between 90 and 110% (Table S1). The recovery rates for As, Cu, and Pb in soil reference material BAM U 115 were 97.7%, 101%, and 104%, respectively (Table S2).

### 2.4. Isotopic and mineralogical analysis

Stable isotopes: total $\delta^{13}C$ and $\delta^{15}N$ stable isotope analysis was conducted on previously homogenized samples at the Institute of Environmental Change and Society in Regina, Canada. Isotopic composition and elemental content were determined using a Costech Elemental Analyzer (ECS 4010) coupled to a Thermo Delta V Plus Isotope Ratio Mass Spectrometer via a Thermo ConFlo IV interface. For calibration, USGS40 and USGS41 standards were employed for both $\delta^{15}N$ and $\delta^{13}C$ measurements. These standards span a broad isotopic range, enabling a two-point calibration correction for each analytical run. The $\delta^{13}C$ values were normalized to the Vienna Pee Dee Belemnite (VPDB) standard, while $\delta^{15}N$ values were normalized relative to atmospheric $N_2$. Quality control measures included bovine liver as a check standard, blank capsules analysed every 10 samples and duplicate samples in all analytical runs. Carbon and nitrogen weight percentages were quantified using a calibration curve established by analysing wheat samples (40 wt% carbon, 2.2 wt% nitrogen) of varying masses (400–1000 μg). Linear regression of carbon and nitrogen peak areas versus sample mass yielded calibration curves with $r^2$ values > 0.998.

Lead Isotopes: all Pb isotope analyses were conducted in a clean room at the MC-ICP-MS Facility, Department of Geological Sciences, University of Cape Town, using a Nu Instruments Plasma3 MC-ICP-S coupled to a Aridus3 desolvating sample introduction system. Approximately 20 mg of each dust sample was weighed into a Savillex PFA beaker, covered with 4 ml of 4:1 concentrated HF:$HNO_3$ acid, closed and placed on a hotplate at 140°C for 48 h. Following complete digestion, samples were opened, dried down and the elemental Pb fraction isolated using Triskem Sr.Spec resin and routine methods (Pin et al., 2014). The Pb isotope compositions were measured in ± 50 ppb Pb solutions and referenced to bracketing analyses of the international isotope standard SRM981 using values for $^{208}Pb/^{204}Pb$, $^{207}Pb/^{204}Pb$, $^{206}Pb/^{204}Pb$ of 36.7219, 15.4963, 16.9405 respectively (Galer & Abouchami, 1998). Instrumental mass fractionation was corrected by addition of SRM997 to standard and samples to give Pb:Tl ratios of ± 10:1, then using the exponential law and a $^{205}Tl/^{203}Tl$ value of 2.3889. Analyses of the reference material JA-2 (andesite) yielded results for $^{208}Pb/^{204}Pb$, $^{207}Pb/^{204}Pb$, $^{206}Pb/^{204}Pb$ of 38.6813 ± 0.0147, 15.6088 ± 0.0043 and 18.4029 ± 0.0032 (2σ, n = 5) in agreement with published data (Tanimizu & Ishikawa, 2006).

Mineralogical analysis: dust samples were examined using a JEOL JSM-IT800 scanning electron microscope (SEM) equipped with an in-lens Schottky field-emission gun and an Oxford Instruments Ultim Max 100 $mm^2$ energy-dispersive X-ray spectroscopy (EDS) detector at the Institute of Earth Sciences, Heidelberg University. All samples were coated with a thin carbon film to avoid surface charging. SEM images were acquired in both secondary electron (SE) and backscattered electron (BSE) modes to document surface topography and compositional variations, respectively. EDS measurements and images were conducted at an accelerating voltage of 18 kV and a beam current of 2.5nA.

For particle classification, analyses focused on grains showing high BSE intensity (i.e., particles with a relatively high average atomic number and therefore enriched in metal-bearing phases). Each particle was classified according to its dominant mineralogical and elemental composition derived from SEM imaging and EDS spectra. Four principal compositional classes were defined. Geological Background (BG), comprising common crustal silicates, carbonates and Ti-bearing minerals. Industrial Legacy Index (ILI), comprising oxidized or weathered metal-bearing phases, including mixed Fe–Cu–Zn oxides, oxy-salts and related secondary minerals. Ore-Specific Index (OSI), comprising primary or secondary ore minerals, particularly Cu–Fe sulphides and associated sulphates. Finally, Anthropogenic Carrier Materials (ACM), comprising particles such as gypsum, glass, halite, barite and related matrices capable of carrying or incorporating metals. Particles with mixed or ambiguous compositions were assigned as “Other”. The relative abundance of each class was calculated as the percentage of classified high-$Z$ particles collected in each sampling site. These classes were used as mineralogical indices and were not interpreted as quantitative source-apportionment fractions. Representative phases and classification criteria are provided in Table S3.

### 2.5. Oxidative Potential

The oxidative potential (OP) of the dust collected was estimated using the dithiothreitol (DTT) assay, which reflects the redox activity of the water-soluble fraction, based on previous methods (Molina et al., 2023). While this approach does not capture the total oxidative capacity, it provides a valuable indicator of the potential for dust particles to generate reactive oxygen species, thereby contributing to adverse health outcomes. The results of the DTT assay were normalized to a positive standard (phenanthrenequinone) to derive a Normalized Index of Oxidant Generation (NIOG).

### 2.6. Zebrafish toxicity assays

Adult zebrafish of the AB strain were reared at the Department of Biosciences, University of Milan. The facility strictly complies with the relevant European and Italian laws, rules, and regulations (i.e., EU Directive 2010/63/EU for animal experiments, Legislative Decree No. 26/2014, Auth. Min. 24/2019-UT, and PG 198,283/2019). All procedures were carried out in accordance with the relevant Italian and

European guidelines and regulations and the ARRIVE guidelines (https://arriveguidelines.org/). Organisms were kept under flow-through conditions at a constant water temperature of 28°C, with a controlled photoperiod of 14/10 h light/darkness. The fish were fed three times daily with finely granulated food (ZM Fish and Food Equipment). Exposure experiments were performed exclusively on embryos and larvae within 120 h post-fertilization (hpf). Based on metal levels, we started with a preliminary range-finding test, exposing embryos to 0.01, 0.1, 1, and 10 mg/L of the potentially more toxic dust, to select an exposure concentration that induces a biological effect. A stock solution (20x) in milliQwater was sonicated for 20 s to assure homogeneous distribution of powder and subsequently diluted in zebrafish water (calcium sulphate 2%, sodium bicarbonate 1%, instant water 1% and methylene blue 0.05%). Embryos were exposed under static conditions following the OECD236 guidelines. No acute effects were observed within 120 hpf at the highest concentration, and for this reason we selected 10 mg/L for the subsequent exposures for toxicity evaluation of all samples. A control group was kept in zebrafish water. Three independent exposure experiments were carried out for every sample. Every 24 h the onset of acute effects, including egg coagulation, lack of somite formation, and absence of heartbeat, as well as sublethal abnormalities, including scoliosis, development delay, edema, and malformations, were recorded. At 72 hpf, a subsample of embryos was assessed for heart rate measurement while the behavioural assay was carried out at the end of the exposure.

Heart rate was assessed in six embryos per treatment. Each embryo was placed in a drop of water on a microscope slide and recorded using a Basler acA1300-60gm GigE camera connected to an optical microscope Videos were recorded for 10 s, and heartbeats were counted over the recording period. The swimming activity was evaluated using the DanioVision™ video tracking system (Noldus IT, Wageningen, Netherlands). For each experimental group we used 6 specimens of the 24 exposed. At the end of exposures, each specimen was put in a single well of a 24-multiplate with 1.5 mL of zebrafish water to undergo 1 cycle of light/dark phases whose duration was 30 min (20 min of dark-10 min of light). Video data were recorded at a sample rate of 30 frames/s via a high-speed infrared camera. The following behavioural parameters were analysed by the software EthoVision XT 11.5 (Noldus IT, Wageningen, Netherlands): the total distance moved, that is the distance travelled by the organism from the previous track to the final one (mm) and the mean mobility, defined by the percentage changes of position (%) of the detected animal between the current and previous tracks.

### 2.7. Statistics and modelling

All statistical analyses were performed in R (version 4.4.0). Continuous variables (metal concentrations, oxidative potential, and zebrafish endpoints) were summarized using medians and interquartile ranges, and no assumptions of normality or homoscedasticity were imposed. Paired comparisons between indoor and outdoor dust at each school were conducted using Wilcoxon signed–rank tests. Differences in zebrafish endpoints (heart rate, locomotor distance, and developmental outcomes) between samples and the regional background were evaluated with Mann–Whitney U tests (Wilcoxon rank–sum tests) for independent samples. All tests were two–sided with a significance threshold of $p < 0.05$. Associations between variables were quantified using Spearman rank correlation coefficients ($\rho$) to evaluate: (i) the coupling between indoor and outdoor metal concentrations across schools; (ii) relationships between oxidative potential and individual metal concentrations; and (iii) the association between school–level heart–rate variability and developmental severity in zebrafish embryos. Simple linear regressions were fitted to describe indoor–outdoor metal relationships at the school level and to visualize compositional trade–offs between mineralogical particle classes. These models were used descriptively; we did not fit multi–predictor regression models or formal interaction terms.

For mineralogical data, mineralogical indices were calculated as the relative abundance of particles in each category (percentage of high–backscatter particles) and treated as continuous variables in correlation and regression analyses. For zebrafish bioassays, the Developmental Severity Index (DSI) was defined for each school as the proportion of exposed embryos exhibiting any non–normal developmental outcome. School–level heart–rate variability was calculated as the standard deviation of heart rate across embryos. The relationship between DSI and heart–rate variability was assessed using Spearman correlation.

Additionally, hourly wind speed (WS2M) and wind direction (WD2M) data for January 2023 were obtained from the NASA POWER archive (MERRA-2 reanalysis) at the study location to provide meteorological context for the sampling campaign. Wind direction frequencies were summarized using 22.5° directional sectors and visualized as wind roses. The proportion of observations originating from the sector encompassing the principal mining district was calculated descriptively to characterize prevailing meteorological conditions during sampling. All figures were generated in R.

## 3. Results

### 3.1. Metals in indoor and outdoor school dust

Concentrations of Cu, As, Pb, and Mo measured in indoor dust closely tracked those measured outdoors at the same schools (Fig. 2, Table 1, Table S4). This close correspondence indicated a minimal attenuation of metal-rich dust between outdoor and indoor classroom environments. Median indoor concentrations were 936 mg $kg^{-1}$ (Cu), 247 mg $kg^{-1}$ (As), 161 mg $kg^{-1}$ (Pb), and 12.9 mg $kg^{-1}$ (Mo), compared with outdoor medians of 1199, 250, 192, and 15.5 mg $kg^{-1}$, respectively (Table 1, Table S4). The corresponding indoor-to-outdoor median ratios (0.78 for Cu, 0.99 for As, 0.83 for both Pb and Mo) indicated limited attenuation of these metals in indoor surface dust, with indoor concentrations only modestly lower than those outdoors. Indoor concentrations exceeded regional desert background levels (Zanetta-Colombo et al., 2024) by approximately five- to sixfold for Cu and Pb and by about one order of magnitude for As and Mo (Table 1, Table S4).

Across schools, indoor and outdoor concentrations were correlated for all four elements (Spearman $\rho = 0.61–0.81$, $p < 0.001$; Table 1). At the school level, indoor–outdoor pairs followed approximately linear relationships, with slopes of 0.94 for As (95% CI: 0.69–1.19), 0.87 for Cu (0.64–1.09), 0.78 for Pb (0.59–0.97) and 0.68 for Mo (0.36–0.99; Table S5), indicating that indoor dust metal concentrations tended to be only modestly lower than outdoors. Wilcoxon signed-rank tests yielded $p$ values of 0.63 for As, 0.053 for Pb and 0.059 for Mo, consistent with small indoor–outdoor differences, whereas Cu concentrations were moderately but significantly higher outdoors than indoors ($p = 0.0002$) (Fig. 2; Table 1). Additionally, wind conditions during the sampling campaign showed prevailing nighttime winds originating from the mining sector (NE/E, 22.5°-112.5°, 60–75%) (Fig. S1).

### 3.2. Stable isotope composition and lead isotopes in indoor dust

Stable carbon and nitrogen isotopes were measured in selected 29 indoor and 12 outdoor dust samples. Indoor dust had a mean $\delta^{13}C$ of $-18.9 \pm 2.1$‰, ranging from $-21.6$ to $-12.0$‰, while outdoor dust had a mean of $-18.0 \pm 2.3$‰, ranging from $-20.8$ to $-12.5$‰. Mean $\delta^{15}N$ values were similar indoors and outdoors, at $6.0 \pm 0.5$‰ and $5.9 \pm 0.4$‰, respectively (Table S5). Indoor $\delta^{13}C$ values fell outside the range reported for modern traffic soot and biomass-burning aerosols (−24 to −34‰; Aguilera & Whigham, 2018) and were consistent with values reported for C4-dominated arid vegetation and associated dust (−16 to −10‰; Cerling et al., 1997). Indoor $\delta^{15}N$ values (5.05 to 7.20‰) exceeded those reported for fresh vehicle emissions ($-2.5 \pm 1.5$‰, Walters et al., 2015) and overlapped with the lower portion of the range reported for aged urban-industrial atmospheric particulate matter (2.3

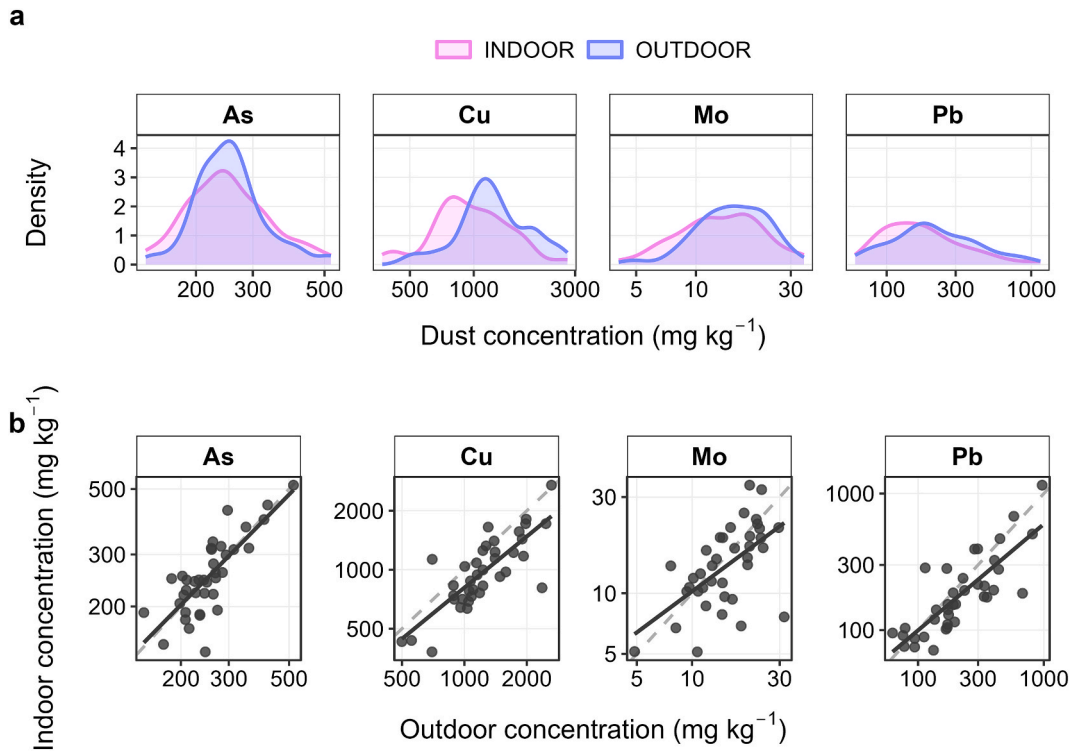


**Fig. 2.** (a) Kernel density distributions of As, Cu, Mo, and Pb concentrations in indoor (pink) and outdoor (blue) surface dust across 38 schools. (b) School-level relationships between outdoor and indoor concentrations. Points represent individual schools, dashed lines indicate the 1:1 relationship, and solid lines show linear fits. Concentration axes are shown on $\log_{10}$ scales and expressed in mg kg$^{-1}$. (For interpretation of the references to colour in this figure legend, the reader is referred to the web version of this article.)

**Table 1**
Indoor and outdoor concentrations, indoor-to-outdoor ratios, and statistical relationships for Cu, As, Pb, and Mo in school dust.

| Metal | Indoor median, mg kg$^{-1}$ | Indoor mean ± SD, mg kg$^{-1}$ | Outdoor median, mg kg$^{-1}$ | Outdoor mean ± SD, mg kg$^{-1}$ | I/O median ratio | Spearman ρ | Regression slope (95% CI) | Paired Wilcoxon p |
|---|---|---|---|---|---|---|---|---|
| Cu | 936 | 1052 ± 454 | 1199 | 1320 ± 503 | 0.78 | 0.78 | 0.87 (0.64–1.09) | 0.0002 |
| As | 247 | 263 ± 82 | 250 | 263 ± 71 | 0.99 | 0.73 | 0.94 (0.69–1.19) | 0.626 |
| Pb | 161 | 225 ± 201 | 192 | 267 ± 202 | 0.83 | 0.81 | 0.78 (0.59–0.97) | 0.053 |
| Mo | 12.9 | 14.8 ± 7.0 | 15.5 | 16.3 ± 6.2 | 0.83 | 0.61 | 0.68 (0.36–0.99) | 0.059 |

Values represent 38 paired indoor and outdoor samples. Concentrations refer to the < 75 μm fraction of school surface dust. I/O denotes the ratio between indoor and outdoor medians. Spearman correlations and regression slopes were calculated using $\log_{10}$-transformed concentrations. All Spearman correlations had $p < 0.001$. Wilcoxon p values derive from paired signed-rank tests.

to 19.7‰; Song et al., 2019; Table S6). These isotopic patterns are compatible with contributions from arid-region material and aged urban–industrial sources, rather than with fresh traffic emissions as the dominant source.

Radiogenic Pb isotopes measured in indoor dust from 38 schools showed narrow ranges for $^{208}Pb/^{207}Pb$ (2.43–2.45) and $^{206}Pb/^{207}Pb$ (1.16–1.18), with mean values of approximately 2.44 ± 0.004 and 1.17 ± 0.003, respectively (Table S7). These values overlapped with the interval defined by local Paleozoic crustal background (Lucassen et al., 2002), Andean ore-derived Pb (Macfarlane & Lechtman, 2016; Puig, 1990), and regional atmospheric deposition fields (Fig. S2, Table S7). These results are consistent with mixed crustal and extractive contributions rather than attribution to a single contemporary emission source.

### 3.3. Mineralogical composition

A total of 9011 indoor dust particles were analysed using SEM-EDS, focusing on grains with high BSE intensity corresponding to high-*Z*, metal-rich fraction (Fig. 3). Particles in this high-*Z* fraction were assigned to four compositional classes used as mineralogical indices: geological background (BG), industrial legacy index (ILI), ore-specific index (OSI), and anthropogenic carrier materials (ACM) (Fig. 3; Table S3 and S8). This fraction roughly comprised 32.9% ILI particles, 23.2% ACM particles, 8.6% OSI particles and 32.3% BG particles; the remaining particles were assigned as "Other" (Fig. 3, Table S7 and S8). BG particles were dominated by silicates, carbonates and Ti-bearing magnetite; ILI particles by metal-rich oxides, oxy-salts and mixed Fe–Cu–Zn phases; ACM particles by gypsum, glass and related matrices; and OSI particles by Cu–Fe sulphides including chalcopyrite, bornite, chalcocite, covellite, digenite, and associated sulphates (Table S8). Across schools, the relative abundance of BG and ILI were negatively associated ($r^2 = 0.59$, $p = 1.6 \times 10^{-6}$; Fig. 3).

### 3.4. Oxidative potential of indoor and outdoor dust

Oxidative potential (OP) was estimated in paired indoor and outdoor dust samples ($n = 38$ per environment). Outdoor samples showed significantly higher OP than indoor samples (median 0.37 vs 0.33 Wilcoxon $p = 0.025$; Fig. 4; Table S9). Indoor OP values ranged from 0.22 to

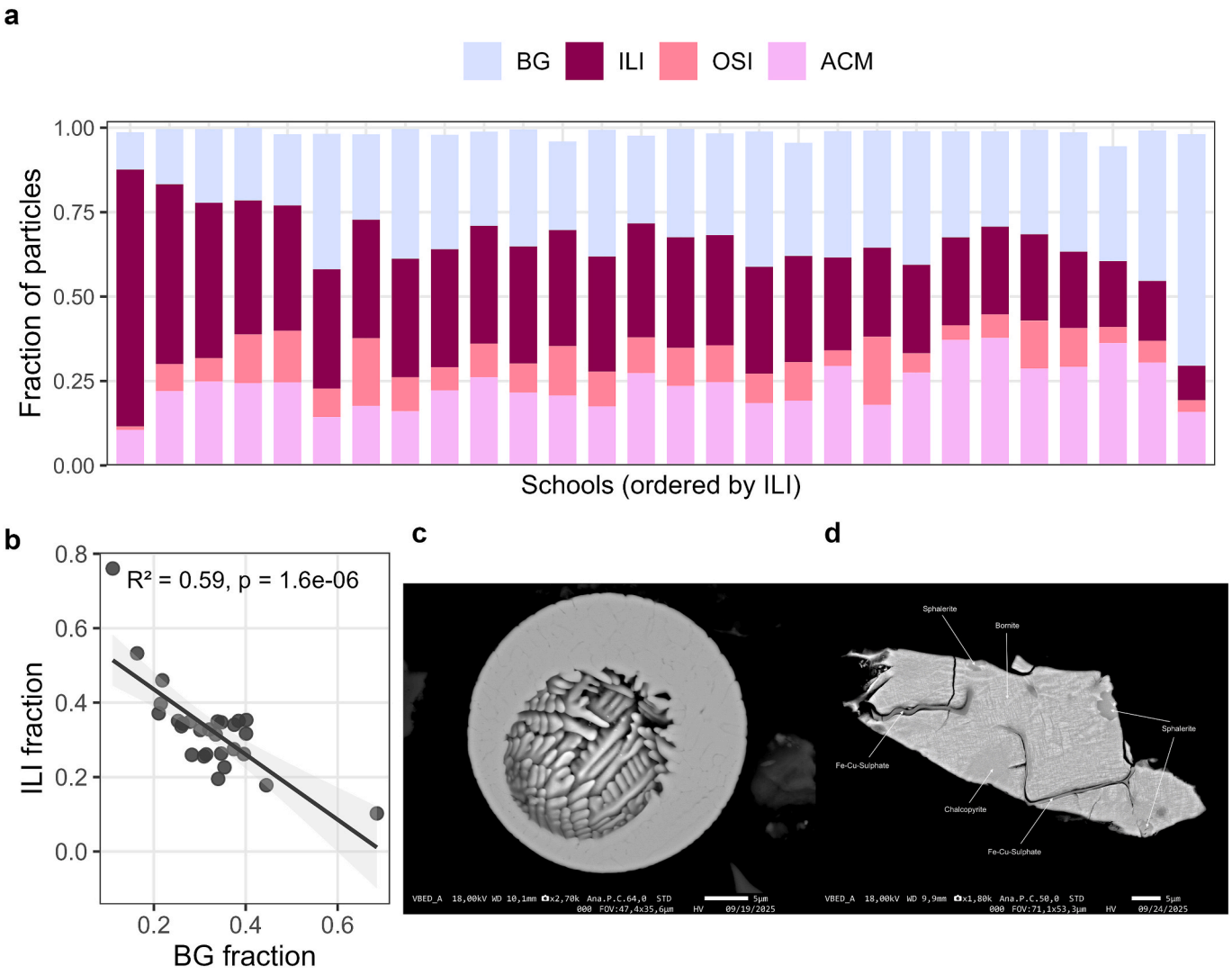


**Fig. 3.** (a) Relative abundances of geological background (BG), industrial legacy index (ILI), ore-specific index (OSI), and anthropogenic carrier materials (ACM) particles in indoor school dust across schools, with bars ordered by ILI abundance. (b) Negative association between BG and ILI relative abundances across schools, with linear fit, $R^2$, and p value. (c–d) Backscattered-electron images illustrating representative high-Z, metal-rich particles, including complex Fe–Cu sulphide aggregates and spheroidal metal-rich grains with textures distinct from common geological particles.

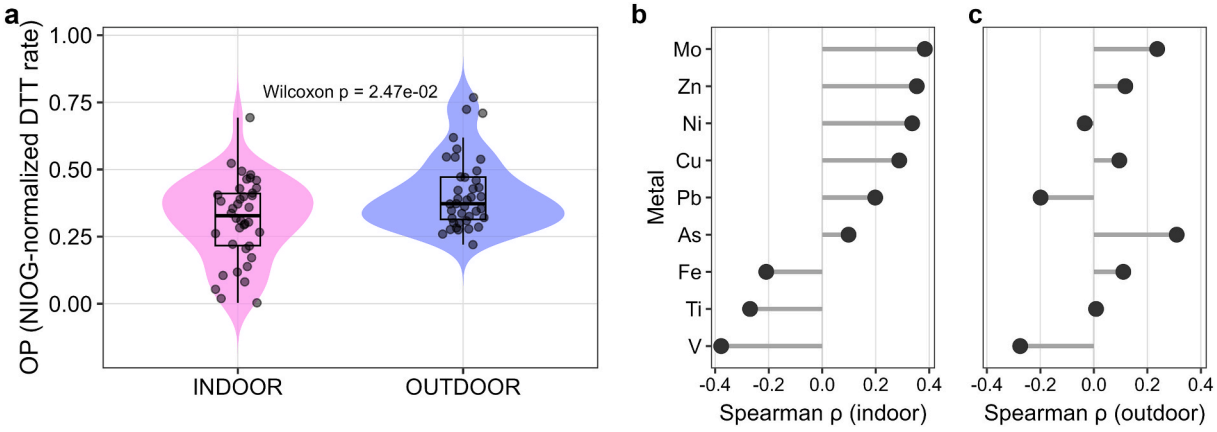


**Fig. 4.** (a) Distribution of NIOG–normalized DTT oxidative potential (OP) in indoor and outdoor dust across 38 schools. (b) Spearman rank correlations between indoor OP and individual metal concentrations. (c) Corresponding Spearman correlations for outdoor OP.

0.41 (interquartile range; Table S9). Across indoor samples, OP was positively correlated with Mo (Spearman $\rho = 0.38$, $p = 0.017$), Zn ($\rho = 0.35$, $p = 0.029$) and Ni ($\rho = 0.34$, $p = 0.039$), and negatively correlated with V ($\rho = -0.38$, $p = 0.019$) (Fig. 4). Correlation with Cu ($\rho = 0.29$, $p$

= 0.080) and other elements ($|\rho|<0.25$) were not significant (Table S10). For outdoor samples, no significant correlations were observed between OP and individual metals (Fig. 4; Table S11).

### 3.5. Zebrafish embryo bioassays

Developmental defects, heart rate, and swimming behaviour were assessed in zebrafish (*Danio rerio*) embryos that were exposed to aqueous extracts from indoor dust samples (Fig. 5). Across all measurements, embryos exposed ($n = 210$) had a median heart rate of 34 beats per 10 s (IQR 33–36), significantly higher than the 29.5 beats per 10 s (IQR 29–30) observed for embryos exposed to control dust ($n = 12$; Wilcoxon rank–sum test, $p = 1.26 \times 10^{-7}$, Fig. 5). On the other hand, total distance travelled by each embryo showed high variability. Median swimming distance was 3130 mm (IQR 2220–4290; $n = 309$) for dust–exposed embryos and 2910 mm (IQR 2280–3720; $n = 36$) for controls, with no evidence of a difference between groups (Wilcoxon rank–sum test, $p = 0.80$; Fig. 5).

Regarding developmental outcomes, median normal development was 84.9% ($n = 27$, IQR 78.5–88.2%), corresponding to a median Developmental Severity Index (DSI) of 15.1% (IQR 11.8–21.5%). The DSI was calculated as the sum of all non-normal acute and sub-lethal developmental outcomes (mortality, edema, malformation, scoliosis and developmental delay), expressed as a percentage of exposed embryos (Table S12, Fig. 5). At the control ($n = 2$), median normal development was 89.0% (range 86.1–91.9%), with a median DSI of 11.0% (range 8.1–13.9%), and there was no evidence of a difference between the samples and the controls for normal development (Wilcoxon rank–sum test, $p = 0.24$). Additionally, heart rate variability (standard deviation across embryos in beats per 10 s) was negatively correlated with DSI (Spearman's $\rho - 0.45$, $p = 0.019$, $n = 27$; Fig. 5 and Table S12). Schools with higher DSI values tended to show lower variability in embryonic heart rate.

## 4. DISCUSSION

### 4.1. Schools within extractive landscapes

Our findings indicate that Cu and Pb outdoor concentrations were about five to six times higher than the regional background, while As and Mo concentrations were about one order of magnitude higher. In this context, indoor concentrations of Cu, As, Pb, and Mo in schools from Calama closely tracked outdoor concentrations, with indoor dust containing about 80% of outdoor levels for Cu, Pb and Mo and nearly identical concentrations for As (Fig. 2; Table S4). The observed indoor–outdoor coupling is compatible with many potential transport and retention processes, including ventilation through open doors and windows, track-in on footwear and clothing, surface deposition, cleaning-related redistribution, and resuspension during routine classroom activity (Diapouli et al., 2008; Liu & Nazaroff, 2003; Thatcher & Layton, 1995; Yuan et al., 2024). Because ventilation and cleaning practices were not systematically recorded, the relative contribution of these mechanisms cannot be resolved from the present data. Similar indoor–outdoor relationships have been documented in mining-affected communities in the Katanga Copperbelt, where indoor dust metal concentrations were comparable to those outdoors, even in simple dwellings (Banza Lubaba Nkulu et al., 2018; Carsi Kuhangana et al., 2026). Our data extend this understanding to an arid, mining-impacted city

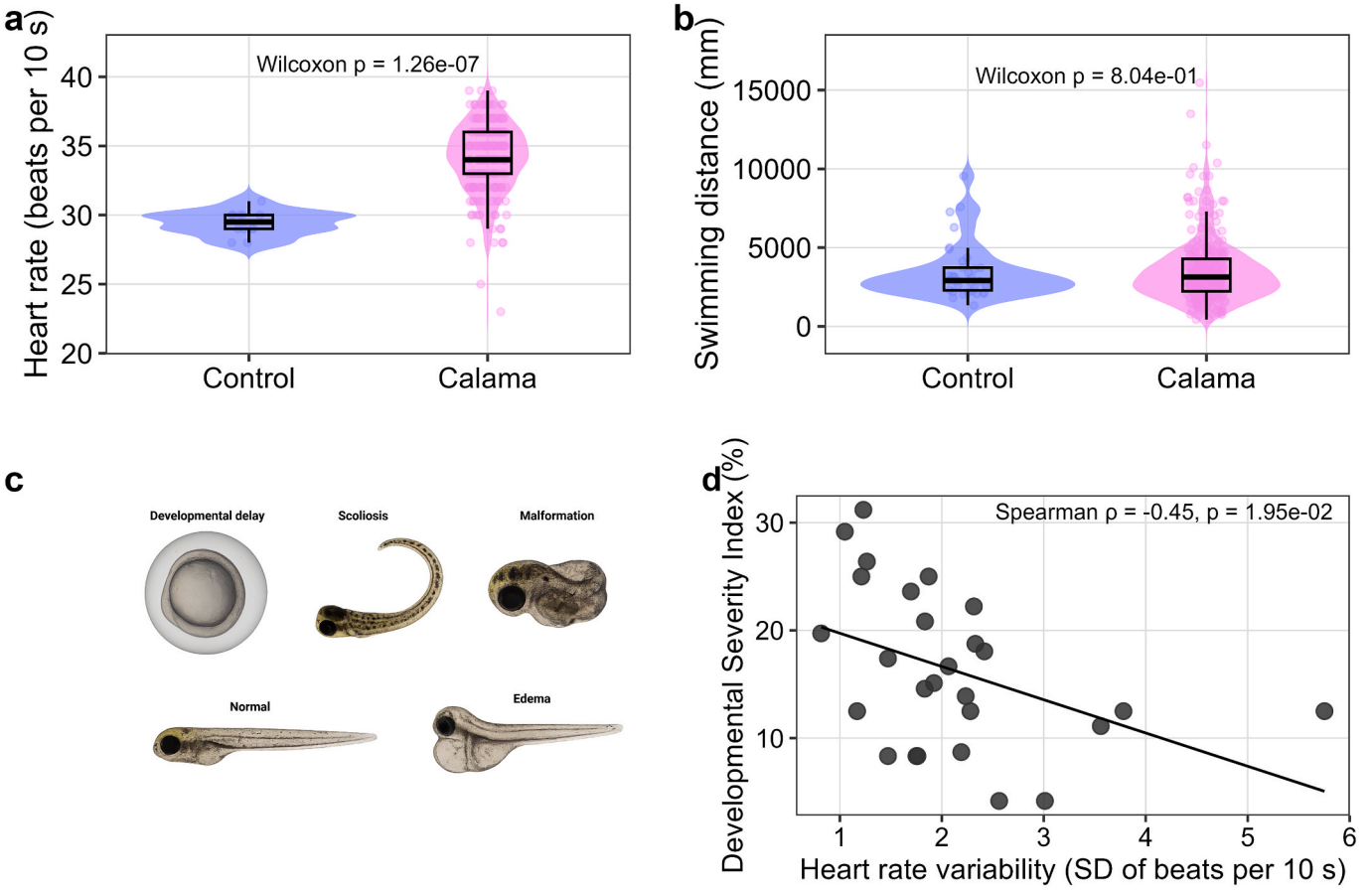


**Fig. 5.** (a) Heart rate of embryos exposed to aqueous dust extracts from Calama schools versus the control site (LGB). (b) Swimming distance as a measure of locomotor activity. (c) Representative phenotypes of normal development and sublethal abnormalities, including developmental delay, scoliosis, malformation, and edema. (d) At the school level, developmental severity index (DSI) decreases with increasing heart–rate variability.

with mostly paved schoolyards, implying that the boundary between outdoor and indoor school spaces is materially weak. Once deposited indoors, dust may persist on surfaces and be repeatedly resuspended during routine classroom activities. Because such resuspended dust can be ingested, mining-derived metals in school dust likely contribute to total exposure alongside dietary pathways highlighted in recent ingestion studies (Carsi Kuhangana et al., 2025, 2026).

### 4.2. Environmental mechanism of exposure

Why do classrooms retain so much mining dust? The answer lies in the physical and chemical nature of mining emissions in desert landscapes. Large-scale Cu extraction, smelting, and tailings handling generate vast quantities of fine metal rich dust (Csavina et al., 2012; Lottermoser, 2010). In arid regions like northern Chile, the lack of rainfall and strong winds may promote long-distance transport and repeated dust resuspension (Morman & Plumlee, 2014). In the Atacama Desert, disturbed soils and tailings heaps release particles that mix geogenic dust with weathered ore residues. These particle mixtures often include secondary minerals, such as metal oxides, oxy-salts and other weathered phases, that are chemically reactive (Nordstrom, 2011).

Wind observations are consistent with the transport pathway also inferred from the Pb isotope signatures, Cu-rich mineral assemblages, and the indoor–outdoor coupling. These independent lines of evidence support the interpretation that atmospheric transport contributes to the delivery of mining-derived particles into indoor environments. In Calama, the wind-driven flux of such dust means that school interiors are continuously replenished with a mix of natural soil and mining legacy materials. Over time, oxidized mining residues progressively accumulated indoors, replacing cleaner background minerals in the particle budget. This dynamic was evident in our analysis, as the share of industrial legacy particles (ILIs) rise, the fraction of background minerals falls.

### 4.3. Indoor dust as a time-integrated archive of extractive legacies

Importantly, indoor dust could reflect a multi-decade record of mining activity, consistent with the persistence of metal-rich particles derived from mine wastes in surrounding landscapes (Hudson-Edwards et al., 2011). Radiogenic Pb isotopes in indoor dust were intermediate between local crustal values and known ore signatures, confirming a mix of crustal and mining-derived Pb. Stable C and N isotopes likewise pointed away from fresh vehicle emissions and toward older soil and industrial sources. Together, the wind, isotopes and mineralogy analysis suggested that mining-era dust has accumulated indoors over time. Single-particle SEM-EDS analysis showed that nearly one third of the metal-bearing fraction consists of oxidized legacy particles enriched in Cu, Fe, Zn, typical of tailings and smelter fallout. Such particles are generated through weathering of mine waste and have been documented in other arid mining districts (Ettler, 2016). Thus, indoor dust can act as a time-integrated archive of extractive residues, forming long-term reservoirs of exposure (Lioy et al., 2002). This could mean that school aged children may be exposed not only to current emissions, but also to the cumulative legacy of mining through contact with and resuspension of settled dust. From a sustainability perspective, this highlights a gap: monitoring ambient outdoor concentrations or recent emissions alone may underestimate both the true exposure burden and the potential impact of mitigation interventions (Filippelli et al., 2020).

### 4.4. Oxidative potential and the limits of bulk concentration metrics

The OP results indicated that indoor dust retained substantial chemical reactivity compared to outdoor dust. Although outdoor samples showed higher median OP values, indoor dust remained strongly redox-active. Importantly, indoor OP correlated with specific metals (Mo, Zn and Ni) but not with total Cu concentrations or overall metal loads. This pattern is consistent with experimental studies showing that OP depends more strongly on metal speciation and particle surface chemistry than on bulk elemental concentrations (Charrier & Anastasio, 2012). In this context, the presence of oxidized legacy particles enriched in mixed metal oxides and salts is likely sustaining the redox activity indoors even where the total metal concentrations are moderately reduced. These results highlight an important limitation of concentration-based exposure metrics. Assessments based solely on bulk metal concentrations in settled dust, such as Pb or Cu, may underestimate the biological reactivity of complex particle mixtures. From a risk-assessment perspective, this distinction is critical. Even when indoor environments comply with regulatory concentration thresholds, particulate mixtures may still retain the capacity to generate oxidative stress through redox-active components. In mining-affected regions, where dust contains complex mixtures of mineral particles and metal-bearing phases, oxidative potential may therefore provide a more functionally relevant indicator of particle hazard than bulk concentration alone.

### 4.5. Sublethal biological responses to dust mixtures

Zebrafish embryo assays provided organism-level preliminary evidence that dust extracts are not biologically inert. Embryos exposed to dust extracts exhibited a significant increase in heart rate, while no significant differences were observed in locomotor behaviour or overall developmental severity. This pattern indicated a physiological response occurring under sublethal exposure conditions. Such responses are consistent with experimental toxicology studies showing that complex chemical mixtures can alter physiological regulation without producing overt malformations or mortality (Kortenkamp & Faust, 2018). Zebrafish are widely used to detect subtle cardiovascular and developmental responses to environmental contaminants (Li et al., 2020), and early-life exposure to metals and oxidative stressors has been shown to influence cardiac function during embryonic development (Bambino & Chu, 2017; Heuer et al., 2024; Hill et al., 2005; Lai et al., 2025; Truong et al., 2011).

Although the specific drivers of the observed cardiac response cannot be isolated in this experiment, the coexistence of elevated embryonic heart rate and measurable oxidative potential suggests a plausible mechanistic link. Redox-active metal phases present in the dust may promote oxidative stress that interferes with ion-channel function or neuroendocrine signalling pathways involved in cardiac regulation. At the same time, the absence of detectable effects on locomotion or gross morphology indicates that these responses occur at a subtle physiological level. From a toxicological perspective, such sublethal responses can be important indicators of environmental stress. Experimental and regulatory research increasingly recognizes that changes in physiological endpoints, including metabolism, cardiovascular function or behaviour, may signal biologically relevant effects even when traditional toxicity endpoints remain unchanged (Kortenkamp & Faust, 2018). In this context, the observed cardiac response supports the interpretation that metal-rich dust mixtures characteristic of mining environments can exert measurable biological effects even under exposure conditions that do not produce overt developmental toxicity.

### 4.6. Study limitations

This study provides a detailed but essentially cross–sectional snapshot of mining–derived metals in school dust. We cannot assess potential seasonal variation in dust loading or metal concentrations. However, the hyper–arid climate and relatively stable mining operations in Calama likely dampen strong seasonal effects. Our school sample is confined to one copper–mining city and may not capture the full socio–economic diversity of schools or conditions in other mining regions. Thus, caution is needed when generalizing beyond similar arid, copper–dominated settings.

We quantified metal concentrations in the $< 75$ μm settled dust

fraction but did not directly characterize airborne particulate matter (e.g., $PM_{10}$ or $PM_{2.5}$). Although all samples were standardized to the < 75 μm fraction, particle-size distributions within this fraction were not determined. Future studies combining settled-dust characterization with indoor air monitoring and modelling of particle deposition and resuspension would provide a more comprehensive assessment of children's exposure.

In addition, settled dust was collected from routinely occupied classrooms without controlling the preceding accumulation period. Consequently, the duration of dust deposition before sampling is unknown and may have varied among schools depending on classroom use and cleaning practices. Likewise, we did not quantify the relative contribution of specific infiltration pathways, such as building-envelope penetration, transport on clothing or footwear, or other mechanisms of particle transfer. We also lacked standardized information on ventilation, occupancy, and cleaning practices, all of which may influence indoor dust accumulation and contribute to variation among schools. These processes could be explored in future studies through targeted observational and tracer-based approaches.

Finally, our toxicity assays were performed in vitro, and we did not collect biomarkers of exposure or health and educational outcomes in schoolchildren, so we cannot make direct inferences about individual–level risk. Nevertheless, our findings align with epidemiological evidence linking metal–rich dust and Pb exposure to adverse health and cognitive effects in children, underscoring the relevance of these dust burdens for public health.

### 4.7. Implications for sustainability, governance and justice

Our findings have broader implications for how the environmental impacts of mining are assessed and governed in the context of the global energy transition. Demand for Cu and other energy-transition minerals is projected to increase substantially in the coming decades as electrification expands and renewable energy systems are deployed at scale (Hund et al., 2023; IEA, 2021; Watari et al., 2019). Meeting this demand will likely intensify extraction in regions that already host large mineral deposits and established mining infrastructure, many of them located in the Global South. While sustainability frameworks for the mining sector have evolved in recent years, they continue to focus primarily on landscape-scale indicators such as land disturbance, water consumption, tailings stability, and greenhouse-gas emissions (Azapagic, 2004; Sovacool et al., 2020). Air pollution is typically assessed through ambient particulate monitoring. Indoor environments, particularly schools where children spend a substantial proportion of their day, are rarely incorporated into environmental impact assessments or long-term monitoring programs (WHO, 2018).

Our results suggest that this omission represents an important gap in current governance frameworks. The strong indoor–outdoor coupling of dust metal concentrations in Calama, together with the persistence of oxidized legacy particles in classroom reservoirs, indicates that school environments are embedded within the broader circulation of mining-derived dust. We use the term “extractive classroom” to describe this condition. In practical terms, this means that regulatory compliance with outdoor air standards does not necessarily translate into reduced metal exposure in child-occupied spaces. Similar mismatches between outdoor indicators and indoor exposure have been highlighted in urban air-quality research, where building infiltration and particle resuspension can maintain elevated pollutant levels indoors despite improvements in ambient air quality (Morawska et al., 2017).

From an environmental justice perspective, this blind spot is consequential. Communities living in extractive regions already experience many of the environmental costs associated with mineral production, including landscape transformation, water depletion and contamination from mining residues (Bebbington et al., 2018). Our findings indicate that an additional and largely overlooked dimension of this burden occurs within school environments. Children in mining-dependent cities could be exposed not only to contemporary emissions but also to the accumulated residues of decades of extraction that persist in indoor dust reservoirs. Because such exposures are rarely measured, they remain largely absent from policy debates and environmental accountability frameworks. This asymmetry reflects a broader challenge identified in discussions of mineral supply chains for the energy transition: the benefits of decarbonization are globally distributed, while the environmental and health risks associated with extraction remain geographically concentrated (Ali et al., 2017; Sovacool et al., 2020).

Addressing this gap requires expanding the scope of environmental monitoring and governance in extractive regions. One practical step would be to incorporate indoor dust measurements in schools into environmental impact assessments and long-term monitoring programs associated with mining operations. Another complementary step would be to establish routine biomonitoring of children in mining-affected communities, as is already done in many jurisdictions for Pb (CDC, 2025). Mine closure and remediation planning could also consider indoor environments as part of the broader legacy of extraction, for example through targeted cleaning programs, improved building envelopes, or enhanced ventilation systems in schools.

Recognizing extractive classrooms as a distinct component of mining landscapes broadens the scope of sustainability of the energy transition (Banza Lubaba Nkulu et al., 2018; Hund et al., 2023; Sovacool et al., 2020). A transition that reduces global carbon emissions while reproducing localized environmental burdens cannot easily be considered equitable (Bainton et al., 2021; Prieto & Zanetta-Colombo, 2024).

## CRediT authorship contribution statement

**Nicolás C. Zanetta-Colombo:** Writing – original draft, Supervision, Investigation, Formal analysis, Data curation, Conceptualization. **Manuel Prieto:** Writing – review & editing, Funding acquisition, Conceptualization. **Carlos A. Manzano:** Writing – review & editing, Funding acquisition, Conceptualization. **Zoë L. Fleming:** Writing – review & editing, Funding acquisition. **Manuel Leiva:** Methodology, Investigation, Funding acquisition. **Javiera Machuca:** Methodology, Investigation. **Lara Nigro:** Methodology, Investigation. **Camilla Della Torre:** Methodology, Investigation. **Anja Eichler:** Methodology, Investigation. **Petrus le Roux:** Methodology, Investigation. **Johanna R.C. Von Holdt:** Methodology, Investigation. **Alexander Varychev:** Methodology, Investigation. **Lucie Tajcmanova:** Methodology, Investigation. **Leah Chibwe:** Methodology, Investigation. **Javier A. Sánchez-Moreno:** Methodology, Investigation. **Christian Scholz:** Methodology, Investigation. **Stefan Rheinberger:** Methodology, Investigation. **Paola Rubilar:** Methodology, Investigation, Formal analysis. **Estela Blanco:** Methodology, Investigation. **Josefa Alarcon-Paredes:** Methodology, Investigation. **Dagmar Brombierstäudl:** Methodology, Investigation. **Benoit Nemery:** Methodology, Investigation, Conceptualization. **Luca Del Giacco:** Methodology, Investigation. **Alberto Diana:** Methodology, Investigation. **Marcus Nüsser:** Methodology, Investigation, Conceptualization.

## Declaration of competing interest

The authors declare that they have no known competing financial interests or personal relationships that could have appeared to influence the work reported in this paper.

## Acknowledgements

We thank Felipe Olivares, Carolina Concha, Luca Toloza, Mariana Mazurett, Nicolás Fierro, and Beatriz Buttazzoni, as well as Javiera Machuca, Nicolás Zanetta-Colombo, and Zoë Fleming, for their weeklong effort in collecting dust samples from schools across Calama, and to Hector Matus and Luis Felipe Sanchez for their support in oxidative potential analyses. We are also grateful to Arturo Bruna, Director of the

Indigenous Department of the Municipality of Calama, for his support in the field logistics. Finally, we extend our appreciation to the school directors and staff for their collaboration and openness in facilitating access to their facilities and for being part of this study. Funding for this research was obtained from the National Agency for Research and Development, Chile (Agencia Nacional de Investigación y Desarrollo, ANID) through grants FONDECYT 1250458, FONDECYT 1251574, FONDECYT 1241485, and FONDECYT 1221951.

## Appendix A. Supplementary data

Supplementary data to this article, consistent of additional analytical and quality control data, summary statistics, dust particles distribution, and atmospheric transport dynamics, can be found online at https://doi.org/10.1016/j.envint.2026.110478.

## Data availability

Data supporting the findings of this study are available from the corresponding author upon reasonable request, subject to ethical, institutional, and community considerations, including the protection of participating schools and communities.

## References

Aguilera, J., Whigham, L.D., 2018. Using the 13C/12C carbon isotope ratio to characterise the emission sources of airborne particulate matter: a review of literature. Isot. Environ. Health Stud. 54 (6), 573–587. https://doi.org/10.1080/10256016.2018.1531854.

Ali, S.H., Giurco, D., Arndt, N., Nickless, E., Brown, G., Demetriades, A., Durrheim, R., Enriquez, M.A., Kinnaird, J., Littleboy, A., Meinert, L.D., Oberhänsli, R., Salem, J., Schodde, R., Schneider, G., Vidal, O., Yakovleva, N., 2017. Mineral supply for sustainable development requires resource governance. Nature 543 (7645), 367–372. https://doi.org/10.1038/nature21359.

Azapagic, A., 2004. Developing a framework for sustainable development indicators for the mining and minerals industry. Journal of Cleaner Production, SME's and Experiences with Environmental Management Systems 12 (6), 639–662. https://doi.org/10.1016/S0959-6526(03)00075-1.

Bainton, N., Kemp, D., Lèbre, E., Owen, J.R., Marston, G., 2021. The energy-extractives nexus and the just transition. Sustain. Dev. 29 (4), 624–634. https://doi.org/10.1002/sd.2163.

Bambino, K., Chu, J., 2017. Zebrafish in Toxicology and Environmental Health. Curr. Top. Dev. Biol. 124, 331–367. https://doi.org/10.1016/bs.ctdb.2016.10.007.

Banza Lubaba Nkulu, C., Casas, L., Haufroid, V., De Putter, T., Saenen, N. D., Kayembe-Kitenge, T., Musa Obadia, P., Kyanika Wa Mukoma, D., Lunda Ilunga, J.-M., Nawrot, T. S., Luboya Numbi, O., Smolders, E., & Nemery, B. (2018). Sustainability of artisanal mining of cobalt in DR Congo. *Nature Sustainability*, *1*(9), 495–504. Doi: 10.1038/s41893-018-0139-4.

Bebbington, A.J., Humphreys Bebbington, D., Sauls, L.A., Rogan, J., Agrawal, S., Gamboa, C., Imhof, A., Johnson, K., Rosa, H., Royo, A., Toumbourou, T., Verdum, R., 2018. Resource extraction and infrastructure threaten forest cover and community rights. PNAS 115 (52), 13164–13173. https://doi.org/10.1073/pnas.1812505115.

Bellinger, D.C., 2013. Prenatal Exposures to Environmental Chemicals and Children's Neurodevelopment: an Update. Saf. Health Work 4 (1), 1–11. https://doi.org/10.5491/SHAW.2013.4.1.1.

Carsi Kuhangana, T., Kasongo Tengwa, G., Roels, L., Mbuyu Ilunga, E., Muta Musambo, T., Musa Obadia, P., Kayembe-Kitenge, T., Katoto, P. D. M. C., Banza Lubaba Nkulu, C., Smolders, E., Hoet, P., & Nemery, B. (2026). Contrasting sources of dietary intake of cobalt and lead in the mining region of Katanga, DR Congo: A duplicate meal study. *Environmental Research*, *295*, 124006. Doi: 10.1016/j.envres.2026.124006.

Carsi Kuhangana, T., Smolders, E., Nemery, B., 2025. Involuntary soil and dust ingestion: much higher estimates in a low-income country than in North America. Environ. Res. 264 (Pt 1), 120352. https://doi.org/10.1016/j.envres.2024.120352.

Cdc, 2025. *Childhood Blood Lead Surveillance: National Data*. Centers for Disease Control and Prevention (CDC).

Cerling, T.E., Harris, J.M., MacFadden, B.J., Leakey, M.G., Quade, J., Eisenmann, V., Ehleringer, J.R., 1997. Global vegetation change through the Miocene/Pliocene boundary. Nature 389 (6647), 153–158. https://doi.org/10.1038/38229.

Charrier, J.G., Anastasio, C., 2012. On dithiothreitol (DTT) as a measure of oxidative potential for ambient particles: evidence for the importance of soluble transition metals. Atmos. Chem. Phys. 12 (19), 9321–9333. https://doi.org/10.5194/acp-12-9321-2012.

Clark, C., Crombie, R., Head, J., van Kamp, I., van Kempen, E., Stansfeld, S.A., 2012. Does Traffic-related Air Pollution Explain Associations of Aircraft and Road Traffic Noise Exposure on Children's Health and Cognition? a Secondary Analysis of the United Kingdom Sample from the RANCH Project. Am. J. Epidemiol. 176 (4), 327–337. https://doi.org/10.1093/aje/kws012.

Cohen, J., Hubbard, H., Özkaynak, H., Thomas, K., Phillips, L., Tulve, N., 2024. Meta-analysis of soil and dust ingestion studies. Environ. Res. 261, 119649. https://doi.org/10.1016/j.envres.2024.119649.

Csavina, J., Field, J., Taylor, M.P., Gao, S., Landázuri, A., Betterton, E.A., Sáez, A.E., 2012. A review on the importance of metals and metalloids in atmospheric dust and aerosol from mining operations. Sci. Total Environ. 433, 58–73. https://doi.org/10.1016/j.scitotenv.2012.06.013.

Diapouli, E., Chaloulakou, A., Mihalopoulos, N., Spyrellis, N., 2008. Indoor and outdoor PM mass and number concentrations at schools in the Athens area. Environ. Monit. Assess. 136 (1–3), 13–20. https://doi.org/10.1007/s10661-007-9724-0.

Ettler, V., 2016. Soil contamination near non-ferrous metal smelters: a review. Applied Geochemistry, Special Issue of Applied Geochemistry on Environmental Impacts of Mining and Smelting 64, 56–74. https://doi.org/10.1016/j.apgeochem.2015.09.020.

Filippelli, G., Anenberg, S., Taylor, M., van Geen, A., Khreis, H., 2020. New Approaches to Identifying and reducing the Global Burden of Disease from Pollution. GeoHealth 4 (4), e2018GH000167. https://doi.org/10.1029/2018GH000167.

Galer, S.J.G., Abouchami, W., 1998. Practical Application of Lead Triple Spiking for Correction of Instrumental Mass Discrimination. Mineral. Mag. 62A (1), 491–492. https://doi.org/10.1180/minmag.1998.62A.1.260.

Gilraine, M., Zheng, A., 2024. JUE insight: Air pollution and student performance in the U.S. J. Urban Econ. 143, 103686. https://doi.org/10.1016/j.jue.2024.103686.

Grandjean, P., Landrigan, P.J., 2014. Neurobehavioural effects of developmental toxicity. The Lancet Neurology 13 (3), 330–338. https://doi.org/10.1016/S1474-4422(13)70278-3.

Heuer, R.M., Falagan-Lotsch, P., Okutsu, J., Deperalto, M., Koop, R.R., Umeh, O.G., Guevara, G.A., Noor, M.I., Covington, M.A., Shelton, D.S., 2024. Therapeutic Efficacy of Selenium Pre-treatment in Mitigating Cadmium-Induced Cardiotoxicity in Zebrafish (Danio rerio). Cardiovasc. Toxicol. 24 (11), 1287–1300. https://doi.org/10.1007/s12012-024-09910-0.

Hill, A.J., Teraoka, H., Heideman, W., Peterson, R.E., 2005. Zebrafish as a Model Vertebrate for investigating Chemical Toxicity. Toxicol. Sci. 86 (1), 6–19. https://doi.org/10.1093/toxsci/kfi110.

Hudson-Edwards, K.A., Jamieson, H.E., Lottermoser, B.G., 2011. Mine Wastes: past, present. Future. Elements 7 (6), 375–380. https://doi.org/10.2113/gselements.7.6.375.

Hund, K.L., Arrobas, D.L.P., Fabregas Masllovet, T.P., Laing, T.J., Drexhage, J.R., 2023. *Minerals for climate Action: the Mineral Intensity of the Clean Energy transition*. World Bank Group. https://documents.worldbank.org/en/publication/documents-reports/documentdetail/en/099052423172525564.

IEA. (2021). *The Role of Critical Minerals in Clean Energy Transitions – Analysis*. https://www.iea.org/reports/the-role-of-critical-minerals-in-clean-energy-transitions.

Kelly, F.J., Fussell, J.C., 2015. Air pollution and public health: Emerging hazards and improved understanding of risk. Environ. Geochem. Health 37 (4), 631–649. https://doi.org/10.1007/s10653-015-9720-1.

Kortenkamp, A., Faust, M., 2018. Regulate to reduce chemical mixture risk. Science 361 (6399), 224–226. https://doi.org/10.1126/science.aat9219.

Lai, Z., Lu, L., Zhang, Y., Zhou, Q., Pu, Y., Yin, L., 2025. Copper exposure induced developmental toxicity and cardiotoxicity in zebrafish. Food Chem. Toxicol. 204, 115660. https://doi.org/10.1016/j.fct.2025.115660.

Landrigan, P.J., Fuller, R., Acosta, N.J.R., Adeyi, O., Arnold, R., Basu, N.N., Baldé, A.B., Bertollini, R., Bose-O'Reilly, S., Boufford, J.I., Breysse, P.N., Chiles, T., Mahidol, C., Coll-Seck, A.M., Cropper, M.L., Fobil, J., Fuster, V., Greenstone, M., Haines, A., Zhong, M., 2018. The Lancet Commission on pollution and health. Lancet (london, England) 391 (10119), 462–512. https://doi.org/10.1016/S0140-6736(17)32345-0.

Lanphear, B.P., Hornung, R., Khoury, J., Yolton, K., Baghurst, P., Bellinger, D.C., Canfield, R.L., Dietrich, K.N., Bornschein, R., Greene, T., Rothenberg, S.J., Needleman, H.L., Schnaas, L., Wasserman, G., Graziano, J., Roberts, R., 2005. Low-level environmental lead exposure and children's intellectual function: an international pooled analysis. Environ. Health Perspect. 113 (7), 894–899. https://doi.org/10.1289/ehp.7688.

Layton, D.W., Beamer, P.I., 2009. Migration of Contaminated Soil and Airborne Particulates to Indoor Dust. Environ. Sci. Technol. 43 (21), 8199–8205. https://doi.org/10.1021/es9003735.

Leppänen, M., Peräniemi, S., Koponen, H., Sippula, O., Pasanen, P., 2020. The effect of the shoeless course on particle concentrations and dust composition in schools. Sci. Total Environ. 710, 136272. https://doi.org/10.1016/j.scitotenv.2019.136272.

Li, R., Zupanic, A., Talikka, M., Belcastro, V., Madan, S., Dörpinghaus, J., vom Berg, C., Szostak, J., Martin, F., Peitsch, M.C., Hoeng, J., 2020. Systems Toxicology Approach for Testing Chemical Cardiotoxicity in Larval Zebrafish. Chem. Res. Toxicol. 33 (10), 2550–2564. https://doi.org/10.1021/acs.chemrestox.0c00095.

Lioy, P.J., Freeman, N.C.G., Millette, J.R., 2002. Dust: a metric for use in residential and building exposure assessment and source characterization. Environ. Health Perspect. 110 (10), 969–983. https://doi.org/10.1289/ehp.02110969.

Liu, D.-L., Nazaroff, W.W., 2003. Particle Penetration through Building Cracks. Aerosol Sci. Tech. 37 (7), 565–573. https://doi.org/10.1080/02786820300927.

Lottermoser, B., 2010. *Mine Wastes*. Springer. https://doi.org/10.1007/978-3-642-12419-8.

Lucassen, F., Harmon, R., Franz, G., Romer, R.L., Becchio, R., Siebel, W., 2002. Lead evolution of the Pre-Mesozoic crust in the Central Andes (18–27°): progressive homogenisation of Pb. Chem. Geol. 186 (3), 183–197. https://doi.org/10.1016/S0009-2541(01)00407-7.

Macfarlane, A.W., Lechtman, H.N., 2016. Andean Ores, Bronze Artifacts, and Lead Isotopes: Constraints on Metal sources in their Geological Context. J. Archaeol. Method Theory 23 (1), 1–72. https://doi.org/10.1007/s10816-014-9225-8.

Molina, C., Manzano, C. A., Toro A., R., & Leiva G, M. A. (2023). The oxidative potential of airborne particulate matter in two urban areas of Chile: More than meets the eye. *Environment International*, *173*, 107866. Doi: 10.1016/j.envint.2023.107866.

Morawska, L., Ayoko, G.A., Bae, G.N., Buonanno, G., Chao, C.Y.H., Clifford, S., Fu, S.C., Hänninen, O., He, C., Isaxon, C., Mazaheri, M., Salthammer, T., Waring, M.S., Wierzbicka, A., 2017. Airborne particles in indoor environment of homes, schools, offices and aged care facilities: the main routes of exposure. Environ. Int. 108, 75–83. https://doi.org/10.1016/j.envint.2017.07.025.

Morman, S.A., Plumlee, G.S., 2014. Dust and Human Health. In: Knippertz, P., Stuut, J.-.-B.-W. (Eds.), *Mineral Dust: A Key Player in the Earth System*. Springer, Netherlands, pp. 385–409. https://doi.org/10.1007/978-94-017-8978-3_15.

Nazaroff, W.W., 2016. Indoor bioaerosol dynamics. Indoor Air 26 (1), 61–78. https://doi.org/10.1111/ina.12174.

Nordstrom, D.K., 2011. Mine Waters: Acidic to Circmneutral. Elements 7 (6), 393–398. https://doi.org/10.2113/gselements.7.6.393.

Pin, C., Gannoun, A., Dupont, A., 2014. Rapid, simultaneous separation of Sr, Pb, and Nd by extraction chromatography prior to isotope ratios determination by TIMS and MC-ICP-MS. J. Anal. At. Spectrom 29 (10), 1858–1870. https://doi.org/10.1039/C4JA00169A.

Plumlee, G.S., Morman, S.A., Ziegler, T.L., 2006. The Toxicological Geochemistry of Earth Materials: an Overview of Processes and the Interdisciplinary Methods used to Understand Them. Rev. Mineral. Geochem. 64 (1), 5–57. https://doi.org/10.2138/rmg.2006.64.2.

Prieto, M., Zanetta-Colombo, N.C., 2024. It's time to talk about the hidden human cost of the green transition. Nature 628 (8008), 502. https://doi.org/10.1038/d41586-024-01084-7.

Puig, A. (1990). Lead Isotopes in the Chilean Ores. In L. Fontboté, G. C. Amstutz, M. Cardozo, E. Cedillo, & J. Frutos (Eds.), *Stratabound Ore Deposits in the Andes* (pp. 749–758). Springer. Doi: 10.1007/978-3-642-88282-1_59.

Rivas, I., Viana, M., Moreno, T., Pandolfi, M., Amato, F., Reche, C., Bouso, L., Àlvarez-Pedrerol, M., Alastuey, A., Sunyer, J., Querol, X., 2014. Child exposure to indoor and outdoor air pollutants in schools in Barcelona, Spain. Environ. Int. 69, 200–212. https://doi.org/10.1016/j.envint.2014.04.009.

Sadrizadeh, S., Yao, R., Yuan, F., Awbi, H., Bahnfleth, W., Bi, Y., Cao, G., Croitoru, C., de Dear, R., Haghighat, F., Kumar, P., Malayeri, M., Nasiri, F., Ruud, M., Sadeghian, P., Wargocki, P., Xiong, J., Yu, W., Li, B., 2022. Indoor air quality and health in schools: a critical review for developing the roadmap for the future school environment. Journal of Building Engineering 57, 104908. https://doi.org/10.1016/j.jobe.2022.104908.

Song, W., Wang, Y.-L., Yang, W., Sun, X.-C., Tong, Y.-D., Wang, X.-M., Liu, C.-Q., Bai, Z.-P., & Liu, X.-Y. (2019). Isotopic evaluation on relative contributions of major NOx sources to nitrate of PM2.5 in Beijing. *Environmental Pollution (Barking, Essex: 1987)*, *248*, 183–190. Doi: 10.1016/j.envpol.2019.01.081.

Sovacool, B.K., Ali, S.H., Bazilian, M., Radley, B., Nemery, B., Okatz, J., Mulvaney, D., 2020. Sustainable minerals and metals for a low-carbon future. Science 367 (6473), 30–33. https://doi.org/10.1126/science.aaz6003.

Sunyer, J., Esnaola, M., Alvarez-Pedrerol, M., Forns, J., Rivas, I., López-Vicente, M., Suades-González, E., Foraster, M., Garcia-Esteban, R., Basagaña, X., Viana, M., Cirach, M., Moreno, T., Alastuey, A., Sebastian-Galles, N., Nieuwenhuijsen, M., Querol, X., 2015. Association between Traffic-Related Air Pollution in Schools and Cognitive Development in Primary School Children: a prospective Cohort Study. PLoS Med. 12 (3), e1001792. https://doi.org/10.1371/journal.pmed.1001792.

Tanimizu, M., Ishikawa, T., 2006. Development of rapid and precise Pb isotope analytical techniques using MC-ICP-MS and new results for GSJ rock reference samples. Geochemical Journal GJ 40, 121–133. https://doi.org/10.2343/geochemj.40.121.

Thatcher, T.L., Layton, D.W., 1995. Deposition, resuspension, and penetration of particles within a residence. Atmos. Environ. 29 (13), 1487–1497. https://doi.org/10.1016/1352-2310(95)00016-R.

Truong, L., Harper, S.L., Tanguay, R.L., 2011. Evaluation of embryotoxicity using the zebrafish model. *Methods in Molecular Biology (Clifton*. N.J.) 691, 271–279. https://doi.org/10.1007/978-1-60761-849-2_16.

Vidal, O., Goffé, B., Arndt, N., 2013. Metals for a low-carbon society. Nat. Geosci. 6 (11), 894–896. https://doi.org/10.1038/ngeo1993.

Walters, W.W., Goodwin, S.R., Michalski, G., 2015. Nitrogen stable isotope composition (δ15N) of vehicle-emitted NOx. Environ. Sci. Technol. 49 (4), 2278–2285. https://doi.org/10.1021/es505580v.

Watari, T., McLellan, B.C., Giurco, D., Dominish, E., Yamasue, E., Nansai, K., 2019. Total material requirement for the global energy transition to 2050: a focus on transport and electricity. Resour. Conserv. Recycl. 148, 91–103. https://doi.org/10.1016/j.resconrec.2019.05.015.

Who, 2018. *WHO Housing and health guidelines*. World Health. Organization. https://www.who.int/publications/i/item/9789241550376.

Yuan, F., Yao, R., Sadrizadeh, S., Awbi, H., Luo, H., Li, B., 2024. The influence of activity patterns and relative humidity on particle resuspension in classrooms. Sci. Total Environ. 946, 173898. https://doi.org/10.1016/j.scitotenv.2024.173898.

Zanetta-Colombo, N.C., Fleming, Z.L., Gayo, E.M., Manzano, C.A., Panagi, M., Valdés, J., Siegmund, A., 2022. Impact of mining on the metal content of dust in indigenous villages of northern Chile. Environ. Int. 169, 107490. https://doi.org/10.1016/j.envint.2022.107490.

Zanetta-Colombo, N.C., Manzano, C.A., Brombierstäudl, D., Fleming, Z.L., Gayo, E.M., Rubinos, D.A., Jerez, Ó., Valdés, J., Prieto, M., Nüsser, M., 2024. Blowin' in the Wind: Mapping the Dispersion of Metal(loid)s from Atacama Mining. GeoHealth 8 (10), e2024GH001078. https://doi.org/10.1029/2024GH001078.